Accuracy Evaluation of Isogray Treatment Planning System for Fields with Regular Shields in Electa Compact Linac

Hamid-Reza Sadoughi (PhD)[1], Masoud Dehestani (MD)[1], Mohsen Khosroabadi (PhD Candidate)[1], Sahar Faraji (PhD Candidate)[2], Mohamad Amin Younessi Heravi (PhD)[1]*

[1]Department of Medical Physics and Radiology, Faculty of Allied Medical Sciences, North Khorasan University of Medical Sciences, Bojnurd, Iran
[2]Radiotherapy Center, Imam Ali Hospital, North Khorasan University of Medical Sciences, Bojnurd, Iran

ABSTRACT

This study evaluates the accuracy of the Isogray Treatment Planning System (TPS) for fields with regular shields on the Elekta Compact linear accelerator, examining absolute and relative dose measurements across field sizes (10×10 cm², 15×15 cm², and 20×20 cm²) and shield coverages (25% and 50%). Absolute dose measurements revealed that the Isogray TPS consistently overestimated doses under shielded conditions, with discrepancies decreasing as the field size increased. In unshielded areas, the TPS demonstrated high accuracy, with dose differences within clinically acceptable limits. Relative dose measurements were evaluated using the gamma index with criteria of 3% dose difference and 3 mm distance-to-agreement. The analysis demonstrated excellent concordance for smaller fields (10×10 cm²), whereas larger fields (15×15 cm² and 20×20 cm²) exhibited significant deviations, particularly beneath the shielding structures and within the penumbral regions. These findings indicate that while the Isogray TPS performs well in open fields, it struggles to accurately model dose distributions in shielded areas, especially for larger fields. The study highlights the need for enhanced algorithms to better account for shielding effects, such as scattered radiation and secondary dose contributions. This work underscores the importance of continuous validation and algorithm optimization to improve the accuracy and reliability of treatment planning systems, ensuring both patient safety and treatment efficacy in complex radiotherapy scenarios.

Keywords

Radiotherapy Planning; Radiation Dosage; Algorithms; Dose Calculation Accuracy; Radiation Protection; Regular Shield

Introduction

In the field of radiotherapy, precision and accuracy in dose delivery are crucial for achieving effective treatment outcomes while minimizing collateral damage to surrounding healthy tissues. Treatment Planning Systems (TPS) play a pivotal role in this process by calculating the optimal dose distribution based on patient-specific anatomy and treatment parameters [1]. Among available TPSs, Isogray is widely utilized in clinical settings for its advanced dose calculation algorithms, though its performance in complex scenarios, such as shielded fields, requires rigorous validation.

Shielded fields refer to radiation fields that incorporate high-density physical barriers designed to protect healthy tissues from unintended radiation exposure, thereby reducing the risks of side effects and

*Corresponding author:
Mohamad Amin Younessi Heravi
Department of Medical Physics and Radiology, Faculty of Allied Medical Sciences, North Khorasan University of Medical Sciences, Bojnurd, Iran
E-mail: a.younessi7@gmail.com

Received: 17 September 2025
Accepted: 13 December 2025

radiation-induced toxicity and overall safety of the treatment [1]. Regular shields, also referred to as simple shields in this context, consist of Cerrobend alloy blocks (a low-melting-point alloy of bismuth, lead, tin, and cadmium) with rectangular geometries positioned within square or rectangular fields. These shields are commonly employed in treatments near critical structures like the spinal cord, kidneys, lungs, or heart, where precise dose control is essential [2]. Materials, such as Cerrobend are favored for their high attenuation properties and ease of molding, with recent studies demonstrating their efficacy in reducing transmission to below 5% for electron energies up to 16 MeV at thicknesses of 10 mm [3, 4]. Similarly, lead-based shields have shown significant cardiac dose reductions (up to 57%) in breast cancer radiotherapy, potentially lowering heart disease risk by 14.8% [5, 6]. Alternative non-toxic composites, such as Polyvinyl Chloride (PVC) heavy transition metal carbide composites, have also emerged as viable lead substitutes for low-energy gamma shielding in healthcare applications [7].

While shielding enhances patient safety, it introduces significant challenges for accurate dose calculation in TPS. Shielding alters the radiation environment by affecting primary beam attenuation, secondary scattering, and dose contributions from adjacent tissues, which can lead to discrepancies between planned and delivered doses [1, 8]. Recent evaluations of Isogray TPS have highlighted acceptable accuracy in open symmetric and asymmetric fields [9] and adjacent radiation fields [10], but limitations persist in wedged or heterogeneous setups, with errors increasing in penumbral and out-of-field regions [11, 12]. Multileaf Collimator (MLC)-based techniques have been proposed as alternatives to traditional Cerrobend blocks for organ protection (e.g., kidneys in abdominal radiotherapy), offering comparable dosimetry with reduced fabrication time and toxicity [13]. However, for scenarios relying on physical shields, TPS algorithms like Collapsed Cone (CC) and Convolution- Fast Fourier Transform (C-FFT) may overestimate or underestimate doses beneath shields due to inadequate modeling of scatter and interface effects [14, 15].

The aim of this study is to evaluate the accuracy of the Isogray TPS in calculating doses for regular shielded fields on the Elekta Compact linear accelerator, by comparing calculated doses with experimental measurements in absolute and relative dosimetry across varying field sizes and shield coverages.

Technical Presentation

This study was conducted to evaluate the accuracy of dose calculations for regular shielded fields. A linear accelerator, the Elekta Compact, was used in this study. This accelerator is designed to produce high-energy photon beams, making it suitable for radiotherapy applications. The evaluated TPS was Isogray, which is specifically designed for calculating dose distributions in radiotherapy. Measurements were carried out in two distinct phases: absolute dose measurement and relative dose measurement.

For absolute dose measurement, a 30×30×30 cm^3 water phantom was used to simulate a clinical environment. A Farmer-type ionization chamber dosimeter (PTW Freiburg) with a sensitive volume of 0.6 cm^3 was employed for dose measurement. Prior to the experiments, the dosimeter was calibrated to ensure accurate dose readings.

The water phantom was positioned at the isocenter of the accelerator. Two points were selected for measurement: one point beneath the shield (Point A) to evaluate the absorbed dose in the shielded region, while the other point was in the open field (Point B) to determine the dose in the unshielded area (Figure 1 visually illustrates these points). The dosimeter was connected to an electrometer (UNIDOS model, PTW Freiburg) for dose readings. After confirming proper alignment, the accelerator was activated to deliver a 6 MV photon beam. Dose measurements were performed three times at each point to ensure statistical validity.

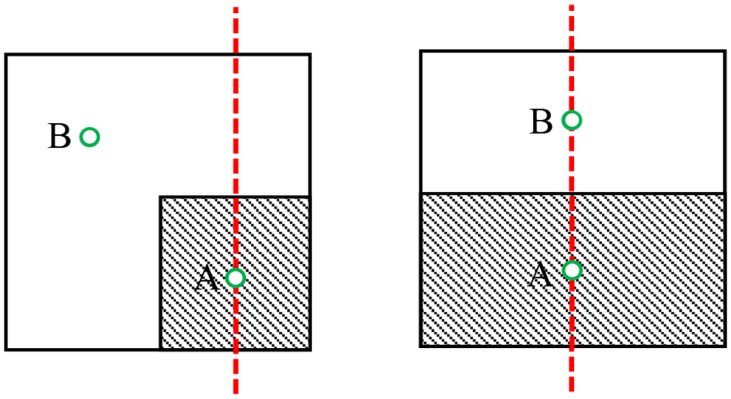

Figure 1: Geometric positioning of the 25% and 50% shields within the radiation field and the paths for dose profile measurements (indicated by dashed lines). The points for absolute dose measurements are labeled as A and B.

For relative dose measurements, a three-dimensional water phantom from PTW was used, which enables precise dose measurements in three dimensions by providing a homogeneous medium for radiation interaction. The water phantom was filled with deionized water to ensure that the conditions closely matched clinical settings. Measurements were conducted using a Semiflex dosimeter (model 31010, PTW) with a sensitive volume of 0.125 cm^3. This small volume is advantageous for recording dose distributions with high spatial resolution, particularly near field edges and shielded regions. Measurements were performed for shielded square fields with dimensions of 10×10 cm^2, 15×15 cm^2, and 20×20 cm^2. Two distinct shield coverage configurations (25% and 50%) were utilized, with the shields composed of Cerrobend, with a uniform thickness of 7 cm. The shields consisted of rectangular blocks covering either 25% or 50% of the field area and were positioned with either corner in the center of the field or edge in the center of the field. The shield was positioned in a manner analogous to patient treatment setups to simulate realistic clinical scenarios. The measurements were carried out for the following field sizes and shield coverages: 1) 10×10 cm^2 field: 25% and 50% shield coverage, 2) 15×15 cm^2 field: 25% and 50% shield coverage, and 3) 20×20 cm^2 field: 25% and 50% shield coverage.

This systematic approach allowed for a comprehensive evaluation of dose distribution under varying field sizes and shield configurations, providing insights into the accuracy and reliability of dose calculations in shielded fields. The shields were positioned in the field using Cerrobend blocks, arranged in geometric configurations similar to those illustrated in the Figure 1. Dose profile measurements were taken precisely through the center of the shield and along the in-plane direction, with the measurement paths indicated by dashed lines in Figure 1.

The following steps were carried out for dose profile measurements: 1) the three-dimensional PTW water phantom was positioned at the isocenter of the Elekta Compact linear accelerator. The phantom was meticulously aligned to ensure the accuracy and precision of the measurements, 2) two Semiflex dosimeters were precisely positioned: one in the measurement field and the other as a reference. To measure the dose within the phantom, data were collected along the in-plane axis. The dosimeter was gradually moved through the water phantom, and doses were recorded at specified intervals (every 2 millimeters), and 3) following the completion of physical measurements, dose calculations for the specified fields were performed using the Isogray TPS. The TPS

computed the expected dose distribution based on input parameters such as beam energy, field geometry, and shield configurations. The extracted data from the TPS included dose values at the same measurement points corresponding to the dosimeter readings in the water phantom.

To evaluate the agreement between the measured dose profiles and the TPS calculations, data analysis was conducted as follows: 1) The measured data were imported into MATLAB; 2) the output from the treatment planning system, which consisted of a three-dimensional dose distribution array, was opened in MATLAB, and the data were extracted at the desired depths and directions; and 3) the gamma index method was employed to quantitatively compare the measured and calculated dose distributions. The gamma index is a widely accepted metric for assessing the agreement between different dosimetric datasets [16].

This systematic approach ensured a rigorous comparison between the experimental measurements and the TPS calculations, providing insights into the accuracy and reliability of the Isogray system in handling shielded fields.

The gamma index analysis was conducted using criteria typically set at a 3% dose difference and a 3 mm Distance-To-Agreement (DTA). These thresholds help define acceptable levels of discrepancy between the measured and calculated results. For each point in the dose profile, the gamma value was computed based on the 3% dose difference and the 3 mm DTA criteria. A statistical analysis of the gamma values was performed, where values less than 1 indicate good agreement. The results were analyzed to evaluate the performance of the TPS under different shield configurations.

Results

Absolute dose measurements recorded under the shield showed that the percentage differences range from 22.22% to 62.50%, with the largest discrepancies observed in the 10×10 cm² field (45.45% for 25% shield and 62.50% for 50% shield), indicating significant overestimation by the TPS. The Standard Deviations (SD=0 Gy) reflect high measurement precision across triplicate readings, suggesting consistent experimental data. These differences decrease with increasing field size, reaching 22.22% for the 20×20 cm² field with 50% shielding.

The data indicate that for field dimensions of 10×10 cm² with shield sizes of 25% and 50%, the measured doses were 0.11 and 0.08 Gy, respectively, while the TPS calculated doses were 0.16 and 0.13 Gy, resulting in differences of 0.05 Gy for both cases. For the 15×15 cm² and 20×20 cm² fields, the differences between the experimental and TPS values ranged from 0.02 Gy to 0.04 Gy, with the smallest difference observed for a 20×20 cm² field with a 50% shield size.

Absolute dose measurements in the open field, the percentage differences are notably smaller, ranging from 0% to 3.91%, with perfect agreement (0%) in the 10×10 cm² field with 25% shielding and minor discrepancies (up to 3.91% for 20×20 cm² with 50% shielding). The low standard deviations (SD ≤0.001 Gy) indicate high precision in the measurements, reinforcing the reliability of the experimental data. These results suggest that the TPS performs robustly in unshielded regions across all field sizes, with differences remaining within typically acceptable clinical thresholds.

Analyzing the measurements for the open areas of the fields reveals a different scenario. In the10×10 cm² field under 25% shield, the measured dose (1.15 Gy) matched perfectly with the TPS value; similarly, in the 50% shield scenario, the measured dose (1.12 Gy) aligned closely with the TPS-calculated dose (1.13 Gy), leading to a minimal difference of just 0.01 Gy. As the field dimensions increased to15×15 cm², the experimental doses were 1.24 Gy and 1.21 Gy for the 25% and 50% shields, respectively, while the TPS predicted doses were slightly higher at 1.26 Gy and 1.25 Gy, resulting in differences of 0.02 Gy and 0.04 Gy. In the largest field, 20×20 cm², the

measurements indicated doses of 1.29 Gy and 1.28 Gy while TPS predictions were 1.34 Gy and 1.33 Gy, respectively, leading to differences of 0.05 Gy for both shielding configurations.

The relative dosimetry results for fields with 25% and 50% shielding were also conducted across the same field dimensions of 10×10 cm², 15×15 cm², and 20×20 cm². These measurements aimed to further evaluate the accuracy of the Isogray TPS in dose distribution calculations under shielded conditions. The dose profiles, represented in Figures 2 and 3, include comparative data for the experimental measurements, TPS predictions using both the CC and C-FFT algorithms, and the corresponding gamma index results to assess the agreement between the measures.

Figures 2 and 3 illustrate the dose profiles for each field dimension with corresponding shield sizes. Each graph displays the experimental dose measurements alongside the TPS-calculated doses from the two algorithms and includes a gamma index analysis.

For the 10×10 cm² field with 25% and 50% shielding, both algorithms demonstrated commendable agreement with the experimental data. The gamma index results for this field indicated high pass rates, suggesting that both the CC and C-FFT algorithms provided precise dose predictions under the influence of shielding. Notably, minor deviations were observed at specific measurement points, particularly at the edges of the shielded region, where dose gradients were steeper.

For the 15×15 cm² field, similar trends were observed, with both TPS algorithms maintaining an acceptable level of conformity with the experimental measurements. The introduction of shielding resulted in slightly increased dose discrepancies compared to the unshielded scenarios, particularly with the 50% shield where

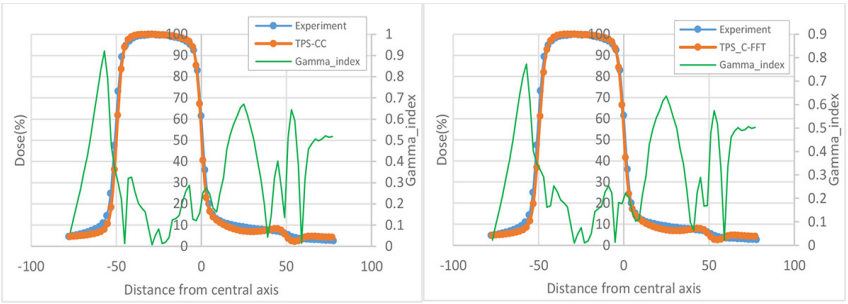

Figure 2: Dose profile for the 10×10 cm² field with 25% shields for (Left) Collapsed Cone and (Right) Convolution- Fast Fourier Transform algorithms in the treatment planning system calculation.

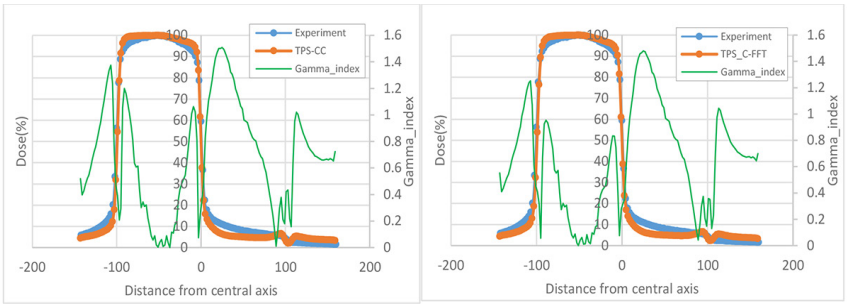

Figure 3: Dose profile for the 20×20 cm² field with 50% shields for (Left) Collapsed Cone and (Right) Convolution- Fast Fourier Transform algorithms in the treatment planning system calculation.

the gamma index indicated a modest decrease in agreement. Nonetheless, overall accuracy remained high, and both algorithms produced favorable gamma results.

In the 20×20 cm^2 field, the effects of shielding became more pronounced, revealing greater variability in the dose profiles. While the overall agreement was still significant, the C-FFT algorithm exhibited larger deviations in specific areas compared to the CC algorithm, which consistently aligned closer to the experimental data. The gamma index analysis for this field reflected a reduction in pass rates, especially in regions near the shield margins, indicating the need for careful calibration and potential adjustments in treatment planning when employing larger fields with substantial shielding.

Table 1 presents the gamma index pass rates, calculated with 3% dose difference and 3 mm distance-to-agreement criteria, for different field sizes, shield configurations, and calculation algorithms (CC and C-FFT). These values illustrate the level of agreement between the measured and TPS-calculated dose profiles and provide an overall assessment of TPS performance.

Discussion

The evaluation of the Isogray TPS on the Elekta Compact linear accelerator showed variations in dose distribution accuracy and consistency for fields with regular shields. Absolute dose measurements and dose profile comparisons provided insight into TPS performance across different field sizes and shielding conditions. These results emphasize the relationship between calculated and measured doses, highlighting both the strengths and limitations of the planning algorithms.

Absolute dose measurements

The results of absolute dose measurements under the shield indicate that, overall, the Isogray TPS tends to overestimate the dose delivered under both 25% and 50% shielding across all field sizes. This consistent overestimation diminishes as the field size increases, suggesting that the TPS may partially account for the increasing complexity of radiation interactions; however, it still falls short in accurately predicting the dose delivered to shielded areas. The observed discrepancies may result from several factors, including the assumption of uniform attenuation by the shielding and potential inaccuracies in modeling the scattering effects due to the geometry and composition of the shields [12, 17, 18]. Large discrepancies between TPS-calculated and measured doses under shielded conditions arise mainly from algorithmic limitations (CC and C-FFT). These algorithms tend to overestimate doses by insufficiently modeling inhomogeneities

Table 1: Gamma index pass rates (%) for the Isogray treatment planning system dose calculations using Collapsed Cone (CC) and Convolution- Fast Fourier Transform (C-FFT) algorithms compared to experimental measurements, evaluated with 3% dose difference and 3 mm distance-to-agreement criteria across different field sizes and shield configurations.

Field dimensions (cm^2)	Shield size (%)	Gamma index pass rate % (Collapsed Cone / Convolution-Fast Fourier Transform algorithms)
10×10	25	100 / 100
	50	100 / 98.6
15×15	25	86.5 / 87.8
	50	86.5 / 89.2
20×20	25	60.8 / 59.5
	50	79.7 / 91.9

and partial volume effects at shield–tissue interfaces, resulting in errors of up to 40% in scattered radiation predictions [18, 19]. Additionally, scattering effects from high-density shielding like Cerrobend contribute to these mismatches by altering secondary radiation contributions are not fully accounted for in the TPS, while setup uncertainties, such as minor misalignments in shield positioning or phantom geometry, can amplify deviations, particularly in larger fields where leakage and patient scatter become more pronounced [20]. In shielded regions, TPS algorithms, like CC and C-FFT often underestimate scattered radiation from collimators and beam modifiers, leading to errors that are exacerbated in heterogeneous environments introduced by high-density materials such as Cerrobend [21].

From a clinical perspective, the percentage differences under the shield (22.22%–62.50%) are substantial and potentially significant. Such overestimations by the TPS may lead to underestimating shielding effectiveness and increase the risk of toxicity to critical organs. This issue is further intensified because, during linear accelerator commissioning, pre-fabricated shields of lesser thickness are typically used instead of custom Cerrobend shields fabricated later. As a result, measured doses are lower than TPS calculations based on commissioning data from these thinner shields. Moreover, as reported by Tahmasebi Birgani et al. [15], repeated use of Cerrobend increases its density and attenuation, producing even lower experimental doses under the shield relative to TPS predictions. In contrast, differences in open areas (0%–3.91%) remain within clinically acceptable limits (<5%), confirming that the TPS provides reliable dose predictions for unshielded regions. These findings highlight the need for improved TPS modeling in shielded scenarios to enhance clinical outcomes [22].

Relative dose measurements

In the 10×10^2 cm² field with 25% and 50% shielding, the results demonstrated an impressive alignment between experimentally measured dose profiles and TPS calculations, with a flawless gamma index pass rate. This outcome suggests that both the CC and C-FFT algorithms performed exceptionally well for smaller field sizes, suggesting that the TPS may have been optimized for managing dose distributions in configurations with limited shielding. The small discrepancies observed in the penumbra region are not unexpected, as penumbral areas are inherently sensitive to measurement variations and can be influenced by factors, such as detector positioning and geometry [23]. It is worth noting that these minor deviations do not undermine the overall efficacy of the TPS in clinically relevant scenarios involving standard 10×10 cm² fields.

Transitioning to the 15×15 cm² field, we encountered a marked change in the performance metrics. While the CC and C-FFT algorithms are again functioned well overall, a significant divergence was noted specifically in the area beneath the shields. The gamma index exceeding one indicates that these TPS algorithms struggled with accurate dose calculations in areas significantly blocked by shielding. This discrepancy may be attributed to several factors, including the increased complexity of dose distribution in larger fields, where scattered radiation and secondary contributions become more prominent, and partial volume effects that degrade prediction accuracy [24]. Additionally, the use of regular shields introduces geometrical complexities that are not fully addressed in the TPS model. In CC algorithms, kernel tilting for inhomogeneities is often inadequate, while in C-FFT algorithms, superposition is limited. These shortcomings lead to mismatches between the planned and the delivered doses [8, 14, 25].

The analysis of the 20×20 cm² field reveals the largest discrepancies between TPS-calculated and measured doses, particularly under shielded regions. This highlights the limitations of the current dose calculation algorithms when applied to larger field sizes. The results indicated that both the CC and C-FFT

algorithms exhibited pronounced discrepancies, not only in the area under the shield but also in the penumbral region. The evident differences between experimental measurements and TPS calculations suggest a systematic challenge for larger fields when implementing shielding. In this context, the TPS may not appropriately accommodate the changes in scattered radiation and secondary dose contributions from adjacent tissue, which can be more influential in broader field geometries due to limitations in beam modeling and inhomogeneity handling [14, 26]. For instance, CC algorithms may overestimate doses in heterogeneous regions by up to 0.9% due to incomplete accounting for tissue interfaces, while C-FFT lacks full 3D kernel superposition, amplifying errors in shielded, larger fields [21, 24].

Table 1 shows the gamma index pass rates, which quantify the discrepancies between measured and calculated doses. For the smaller 10×10 cm² field, both CC and C-FFT algorithms achieved excellent agreement (100% in most cases) under 25% and 50% shielding. This outcome reflects the TPS optimization for limited shielding configurations. However, pass rates decline notably in larger fields, dropping to as low as 59.5% for the 20×20 cm² field with 25% shielding using C-FFT, underscoring the algorithms' challenges in modeling scattered radiation and penumbral effects in broader geometries; interestingly, the C-FFT algorithm shows slightly higher pass rates in some 50% shielded scenarios (e.g., 91.9% vs. 79.7% for CC in 20×20 cm²), suggesting differential handling of attenuation and superposition between the two methods.

The overall performance of the Isogray TPS has demonstrated robustness for open field scenarios while highlighting significant challenges in dose prediction under shielded conditions, especially as the field size increases. The systematic overestimation of doses beneath the shields calls for further investigation into refining shielding models used within the TPS. The clinical use of manual shields such as Cerrobend has declined with the advent of MLCs [27-29]. MLCs provide precise beam shaping, greater efficiency, and reduced toxicity without custom block fabrication [27-29]. However, manual shields remain relevant in certain cases, including hypofractionated treatments or when MLC limitations (e.g., leaf width in complex geometries) require additional protection [30-32]. To ensure optimal patient safety and treatment efficacy, continuous validation against clinical measurements is critical, particularly for complex treatment scenarios. Enhanced algorithms that better account for shielding effects are essential for accurate treatment planning. They ensure radiation therapy remains safe and effective across all prescribed field sizes.

Conclusion

The comprehensive evaluation of the Isogray TPS, in conjunction with experimental absolute dose measurements, has revealed important insights into its performance across different field sizes and shielding configurations. Our findings demonstrate that while the TPS exhibits commendable accuracy in predicting dose distributions in unshielded areas, it struggles with overestimating doses delivered under shielding conditions, particularly in larger fields. This inconsistency highlights the complexities involved in accurately modeling radiation interactions in the presence of shielding, which can significantly impact treatment efficacy and patient safety. In summary, this research identifies both strengths and weaknesses of the Isogray TPS, showcasing its utility while also highlighting critical areas for improvement. To enhance the reliability and precision of TPS outputs in clinical settings, particularly with challenging geometries, further research is essential.

Some suggestions for future research are algorithm enhancement for more accurately modeling the physical interactions of radiation with shielding materials. This could involve advanced Monte Carlo simulations that consider heterogeneous tissue compositions and varying geometric configurations to provide a

more precise representation of dose distributions under shields. Conducting a comparative analysis of multiple treatment planning systems for the same set of conditions (field sizes, shielding types, and geometries). Future studies should also examine a wider range of field sizes and shielding configurations, including irregular and customized designs.

By pursuing research on algorithm enhancement, Monte Carlo simulations, and comparative analyses of treatment planning systems, the field of radiation therapy can enhance the effectiveness of treatment planning systems, ultimately leading to improved outcomes for patients undergoing radiation treatment.

Acknowledgment

We would like to thank all the people who participated in the study and helped us collect data.

Authors' Contribution

HR. Sadoughi contributed to the conceptualization, methodology design, software development, formal analysis, original draft writing, project administration, and data visualization. M. Dehestani was responsible for the investigation. M. Khosroabadi contributed to data curation and investigation. S. Faraji participated in the investigation. MA. Younessi Heravi contributed to validation and data curation. All authors reviewed and edited the manuscript and approved the final version for submission.

Funding

This work was conducted at North Khorasan University of Medical Sciences under project number IR. NKUMS.4000263.

Conflict of Interest

None

References

1. Khan FM, Gibbons JP. Khan's The Physics of Radiation Therapy. 5th ed. Philadelphia: Lippincott Williams & Wilkins; 2014.
2. Khan FM, Sperduto PW, Gibbons JP. Khan's Treatment Planning in Radiation Oncology. 5th ed. Philadelphia: Lippincott Williams & Wilkins; 2021.
3. Farajollahi AR, Bouzarjomehri F, Kiani M. Comparison between Clinically Used Irregular Fields Shielded by Cerrobend and Standard Lead Blocks. *J Biomed Phys Eng.* 2015;**5**(2):77-82. PubMed PMID: 26157733. PubMed PMCID: PMC4479389.
4. Penyu MZ, Zakaria NS, Wahabi JM, Mansor MF. Effectiveness of cerrobend alloy metal as prominent shielding material for electron beam therapy. *Radiat Phys Chem.* 2025;**236**:112857. doi: 10.1016/j.radphyschem.2025.112857.
5. Chiu HW, Lai LH, Ting CY. A dosimetric analysis of reduction cardiac dose with lead shielding in breast cancer radiotherapy. *Appl Sci.* 2021;**11**(20):9686. doi: 10.3390/app11209686
6. Shah C, Badiyan S, Berry S, Khan AJ, Goyal S, Schulte K, et al. Cardiac dose sparing and avoidance techniques in breast cancer radiotherapy. *Radiother Oncol.* 2014;**112**(1):9-16. doi: 10.1016/j.radonc.2014.04.009. PubMed PMID: 24813095.
7. Hadjal A, Saim A, Dib AS, Tebboune A, Belkaid N. T1-P21: Evaluation of Gamma-Rays Shielding Properties of PVC/Heavy Transition Metal Carbides Composites in Healthcare Applications. 4th International Conference on Radiations And Applications; Algeria: ICRAA; 2025. p. 90.
8. Kry SF, Bednarz B, Howell RM, Dauer L, Followill D, Klein E, et al. AAPM TG 158: Measurement and calculation of doses outside the treated volume from external-beam radiation therapy. *Med Phys.* 2017;**44**(10):e391-429. doi: 10.1002/mp.12462. PubMed PMID: 28688159.
9. Naghiloo M, Khosroabadi M, Abaspour A, Reza H. Accuracy Evaluation of Isogray TPS Dose Calculations in Symmetric and Asymmetric Fields of the Elekta Compact Linear Accelerator. *Med Sci.* 2021;**13**(3):15-22. doi: 10.29252/nkjmd-13032.
10. Rasouli A, Arani MN, Aliasgharzadeh A, Farhood B. Evaluation of dose calculation accuracy of a commercial radiotherapy treatment planning system for adjacent radiation fields. *J Radiother Pract.* 2023;**22**:e93. doi: 10.1017/S146039692300016X.
11. Raghavi S, Sadoughi HR, Ravari ME, Mansoury MT, Behmadi M. Accuracy evaluation of dose calculation of ISOgray treatment planning system in wedged treatment fields. *International Journal of Radiation Research.* 2024;**22**(2):303-8. doi: 10.61186/ijrr.22.2.303.
12. Bahreyni Toosi MT, Momeni S, Soleymanifard Sh, Gholamhosseinian H. Evaluation of Dose Calculation Accuracy of Isogray Treatment Planning System in Craniospinal Radiotherapy. *Iran J Med Phys.* 2018;**15**:231-6. doi: 10.22038/ijmp.2018.27332.1291.
13. Parvaii W, Kakavand GM, Hadisinia T. Implementa-

tion of MLC-based techniques for kidney protection as isolated organs during radiotherapy of abdominal malignancies. *J Ilam Univ Med Sci.* 2025;**33**(2):1-2.

14. Ojala J. Monte Carlo simulations in quality assurance of dosimetry and clinical dose calculations in radiotherapy [dissertation]. Tampere: Tampere University of Technology; 2014. Available from: https://trepo.tuni.fi/bitstream/handle/10024/225191/ojala.pdf?sequence=1&isAllowed=y.
15. Tahmasebi Birgani MJ, Farhadi Birgani F, Behrooz MA, Ali Behrooz SM, Maghsoodi Niya F. Evaluation of Change in Attenuation Coefficient of Cerrobend Block Used for Radiation Protection of Healthy Tissues in Megavoltage Photon Radiation Therapy after Multiple Melting. *Jundishapur Sci Med J.* 2014;**13**(3):266-74.
16. Low DA. Gamma Dose Distribution Evaluation Tool. *J Phys Conf Ser.* 2010;**250**(1):012071. doi: 10.1088/1742-6596/250/1/012071.
17. Al-Ghorabie FH, Al-Lyhiani SS, Natto SS. EGSnrc computer modelling of megavoltage x-rays transmission through some shielding materials used in radiotherapy. *J Radiother Pract.* 2010;**9**(4):223-36. doi: 10.1017/S1460396910000129.
18. Huang JY, Followill DS, Wang XA, Kry SF. Accuracy and sources of error of out-of field dose calculations by a commercial treatment planning system for intensity-modulated radiation therapy treatments. *J Appl Clin Med Phys.* 2013;**14**(2):4139. doi: 10.1120/jacmp.v14i2.4139. PubMed PMID: 23470942. PubMed PMCID: PMC5714363.
19. Mahmoudi G, Farhood B, Shokrani P, Amouheidari A, Atarod M. Evaluation of the photon dose calculation accuracy in radiation therapy of malignant pleural mesothelioma. *J Cancer Res Ther.* 2018;**14**(5):1029-35. doi: 10.4103/0973-1482.187284. PubMed PMID: 30197343.
20. Farhood B, Ghorbani M. Dose Calculation Accuracy of Radiotherapy Treatment Planning Systems in Out-of-Field Regions. *J Biomed Phys Eng.* 2019;**9**(2):133-6. doi: 10.31661/jbpe.v0i0.901. PubMed PMID: 31214518. PubMed PMCID: PMC6538908.
21. Mohammadi K, Hassani M, Ghorbani M, Farhood B, Knaup C. Evaluation of the accuracy of various dose calculation algorithms of a commercial treatment planning system in the presence of hip prosthesis and comparison with Monte Carlo. *J Cancer Res Ther.* 2017;**13**(3):501-9. doi: 10.4103/0973-1482.204903. PubMed PMID: 28862217.
22. Golestani A, Houshyari M, Mostaar A, Arfaie AJ. Evaluation of dose calculation algorithms of Isogray treatment planning system using measurement in heterogeneous phantom. *Rep Radiother Oncol.* 2015;**2**(3):e5320.oi: 10.17795/rro-5320.
23. García-Vicente F, Béjar MJ, Pérez L, Torres JJ. Clinical impact of the detector size effect in 3D-CRT. *Radiother Oncol.* 2005;**74**(3):315-22. doi: 10.1016/j.radonc.2004.10.012. PubMed PMID: 15763313.
24. Oncology Medical Physics. Dose Calculation Algorithms. 2025. Available from: https://oncologymedicalphysics.com/dose-calculation-algorithms/.
25. Papanikolaou N, Stathakis S. Dose-calculation algorithms in the context of inhomogeneity corrections for high energy photon beams. *Med Phys.* 2009;**36**(10):4765-75. doi: 10.1118/1.3213523. PubMed PMID: 19928107.
26. Lee BI, Boss MK, LaRue SM, Martin T, Leary D. Comparative study of the collapsed cone convolution and Monte Carlo algorithms for radiation therapy planning of canine sinonasal tumors reveals significant dosimetric differences. *Vet Radiol Ultrasound.* 2022;**63**(1):91-101. doi: 10.1111/vru.13039. PubMed PMID: 34755417.
27. Cheng CW, Das IJ, Steinberg T. Role of multileaf collimator in replacing shielding blocks in radiation therapy. *Int J Cancer.* 2001;**96**(6):385-95. doi: 10.1002/ijc.1038. PubMed PMID: 11745510.
28. Boyer A, Biggs P, Galvin J, Klein E, LoSasso T, Low D, et al, AAPM Radiation Therapy Committee, Basic applications of multileaf collimators. Alexandria, VA: American Association of Physicists in Medicine; 2001.
29. Mahani L, Kazemzadeh A, Saeb M, Kianinia M, Akhavan A. The Efficacy of Multi-Leaf Collimator in the Reduction of Cardiac and Coronary Artery Dose in Left-Sided Breast Cancer Radiotherapy. *Adv Biomed Res.* 2023;**12**:89. doi: 10.4103/abr.abr_342_21. PubMed PMID: 37288034. PubMed PMCID: PMC10241641.
30. Yoganathan SA, Mani KR, Das KJ, Agarwal A, Kumar S. Dosimetric effect of multileaf collimator leaf width in intensity-modulated radiotherapy delivery techniques for small- and large-volume targets. *J Med Phys.* 2011;**36**(2):72-7. doi: 10.4103/0971-6203.79690. PubMed PMID: 21731222. PubMed PMCID: PMC3119955.
31. Fast MF, Kamerling CP, Ziegenhein P, Menten MJ, Bedford JL, Nill S, Oelfke U. Assessment of MLC tracking performance during hypofractionated prostate radiotherapy using real-time dose reconstruction. *Phys Med Biol.* 2016;**61**(4):1546-62. doi: 10.1088/0031-9155/61/4/1546. PubMed PMID: 26816273. PubMed PMCID: PMC5390952.
32. Kamerling CP, Fast MF, Ziegenhein P, Menten MJ, Nill S, Oelfke U. Real-time 4D dose reconstruction for tracked dynamic MLC deliveries for lung SBRT. *Med Phys.* 2016;**43**(11):6072. doi: 10.1118/1.4965045. PubMed PMID: 27806589. PubMed PMCID: PMC5965366.